Climate Dynamics (2003) 20: 415–429
DOI 10.1007/s00382-002-0283-3

G.J. Boer · B. Yu

Climate sensitivity and response

Received: 23 April 2002 / Accepted: 21 August 2002 / Published online: 26 October 2002

Abstract Results from climate change simulations indicate a reasonably robust proportionality between global mean radiative forcing and global mean surface air temperature response. The "constant" of proportionality is a measure of the overall strength of climate feedback processes and hence of global climate sensitivity. Geographically, however, temperature response patterns are generally not proportional to, nor do they resemble, their parent forcing patterns. Temperature response patterns, nevertheless, exhibit a remarkable additivity whereby the sum of response patterns for different forcings closely resembles the response pattern for the sum of the forcings.

The geographical distribution of contributions to the climate sensitivity/feedback are obtained diagnostically from simulations with the Canadian Centre for Climate Modelling and Analysis (CCCma) coupled global climate model (GCM). There is positive feedback over high-latitude oceans, over northern land areas, and over the equatorial Pacific. The remaining regions over oceans and tropical land areas exhibit negative feedback. The feedback results are decomposed into components associated with short-and longwave radiative processes and in terms of cloud-free atmosphere/surface and cloud feedbacks. While the geographic pattern of the feedbacks may generally be linked to local processes, all feedback processes display regions of both positive and negative values (except for the solar atmosphere/surface feedback associated with the retreat of ice and snow which is positive) and all vary from place to place so that there is no simple physical picture that operates everywhere. The stable geographical pattern of the feedback is a consequence of the balance between local physical processes rather than the dominance of a particular process.

The feedback results indicate that, to first order, temperature response patterns are determined by the geographical pattern of local feedback processes. The feedback processes act to localize forcing changes and to generate temperature response patterns which depend firstly on the pattern of feedbacks and only secondarily on the pattern of the forcing. The geographical distribution of feedback processes can be regarded as a feature of the climate model (and by inference of the climate system) and not (or only comparatively weak) functions of forcing and climate state. An illustrative model is able to reproduce qualitatively the kinds of forcing/temperature response behavior seen in the CCCma GCM including the quasi-independence of forcing and response patterns, the additivity of temperature response patterns, and the resulting "non-constancy" of the global climate sensitivity.

G.J. Boer (✉) · B. Yu
Canadian Center for Climate Modelling and Analysis,
Meteorological Service of Canada, PO Box 1700,
Victoria, B.C. V8W 2Y2, University of Victoria, Canada
E-mail: george.boer@ec.gc.ca

1 Introduction

Projections of future climate change are typically obtained using coupled global climate models (GCMs) which "translate" changes in the atmospheric concentration of greenhouse gases (GHGs) and aerosol loadings into changes in climate. To the extent that the models embody the controlling physical principles of the climate system the resulting simulated climate change will be realistic and useful (provided, of course, that the concentration scenarios themselves are pertinent). The climate system is complex so that cause and effect is difficult to untangle and this is equally true for the results of climate model simulations. In particular, the response of the climate system (and models of the climate system) to natural (e.g. solar variations, volcanos) or anthropogenic (e.g. GHG emissions, sulfate aerosols) perturbations to the system is not immediate as to magnitude or pattern.

One approach to characterizing climate model and/or climate system response relates the global mean *radiative*

forcing associated with a perturbation of the system to the resulting global mean temperature change after the system reaches a new equilibrium. The constant of proportionality connecting radiative forcing to temperature change is a measure of the strength of the *climate feedback* processes operating in the system and hence of *climate sensitivity*. A reasonably robust linear connection between radiative forcing and climate response allows some aspects of climate change to be estimated from radiative forcing estimates alone, without the costly computations involved in simulations with a full GCM.

We investigate three aspects of climate sensitivity and response namely: (Pl) the proportionality between global average forcing and global average temperature response which is largely independent of both the nature of the forcing and its geographical pattern; (P2) the notable *lack* of correlation between the geographical pattern of the forcing and the geographical pattern of temperature response; and (P3) the remarkable additivity of response patterns whereby the sum of the temperature response patterns for a number of different forcings is very nearly the response pattern of the sum of the forcings.

Local contributions to climate sensitivity are analyzed in the context of the energy budget of the system. The behaviour of the Canadian Centre for Climate Modelling and Analysis (CCCma) coupled global climate model simulations of forced climate change is investigated in this context and a feedback/response hypothesis proposed to explain the temperature response of our and other GCMs to radiative forcing change. The hypothesis is that, to first order, temperature response patterns are determined by the geographical pattern of local feedback processes. These robust feedback processes act to "localize" the response to both local and also to remote forcing changes, which are felt locally via system transport processes. The local feedback processes thereby generate a temperature response pattern which is determined primarily by the pattern of feedbacks and only secondarily by the pattern of forcing.

Both GCM results and those of an illustrative model demonstrate how this qualitatively accounts for the "generic" temperature response pattern that results from modestly different forcing patterns as well as the less generic responses that are found when forcing patterns have large gradients. The additivity of temperature response patterns follows from the hypothesis but the "constancy" of the global mean climate sensitivity, and its independence from the forcing pattern, is seen to be only approximate.

2 Climate forcing and response

For our purposes we distinguish the internal components of the climate system as represented by the CCCma coupled climate model (Flato et al. 2000) as those components which are predicted or calculated (wind, temperature, precipitation rate, snow cover, salinity etc.) from the external components which are specified (topography, solar constant, atmospheric GHG concentration, aerosol loading, etc.).

A change in an external parameter of the system will result in a change in climate. For instance an increase in GHG concentration in the atmosphere will modify the radiative balance and a change in mean temperature and in other climate statistics will result. The change is forced, so to say, by the effect of the GHGs on the radiative stream. A relationship between the radiative forcing due to a given change in an external parameter and the resulting surface air temperature change, after the system has come to a new equilibrium in balance with the changed external parameters, may be written in the form

$$\langle T' \rangle = \hat{s} \langle f \rangle = \langle f \rangle \hat{\lambda} \tag{1}$$

where $\langle T' \rangle$ is the global mean (indicated by angular brackets) change (indicated by the prime) in surface air temperature and $\langle f \rangle$ is the global mean radiative forcing. The transfer function $\hat{s}$ is termed the sensitivity parameter, and its inverse $\hat{\lambda}$ the feedback parameter, where the caret is used to indicate that changes in globally averaged temperature and forcing are being considered. Climate model simulations indicate that $\hat{s} = 1/\hat{\lambda}$ is approximately constant and independent of the magnitude and pattern of the forcing.

We relate the feedback/sensitivity parameter and the radiative forcing to the global energy budget, investigate the processes which determine the geographical distribution of contributions to the global feedback/sensitivity, and discuss how this determines the geographical pattern of the temperature response in simulations with the CCCma climate model.

3 Climate change simulations

A range of climate change simulations have been performed with the CCCma coupled general circulation model. The coupled model, control climate, forcing scenarios, and the simulated climate change from 1900 to 2100 are detailed in Flato et al. (2000), and Boer et al. (2000a,b). The atmospheric component of the CCCma coupled general circulation model (GCM) is a spectral model with T32L10 triangular resolution. The oceanic component is a version of the MOM ocean model (Pacanowski et al. 1993) at a resolution of 1.8° × 1.8°L29.

Simulation results are available from a control run (of 1000-years) and three independent transient climate change simulations for the period 1900–2100 forced with historical and projected greenhouse gas concentration and aerosol loadings. Two additional simulations (both of 1000-years) are performed where the forcing is "stabilized" at 2050 and 2100 values and the system allowed to approach a new equilibrium with this now constant forcing.

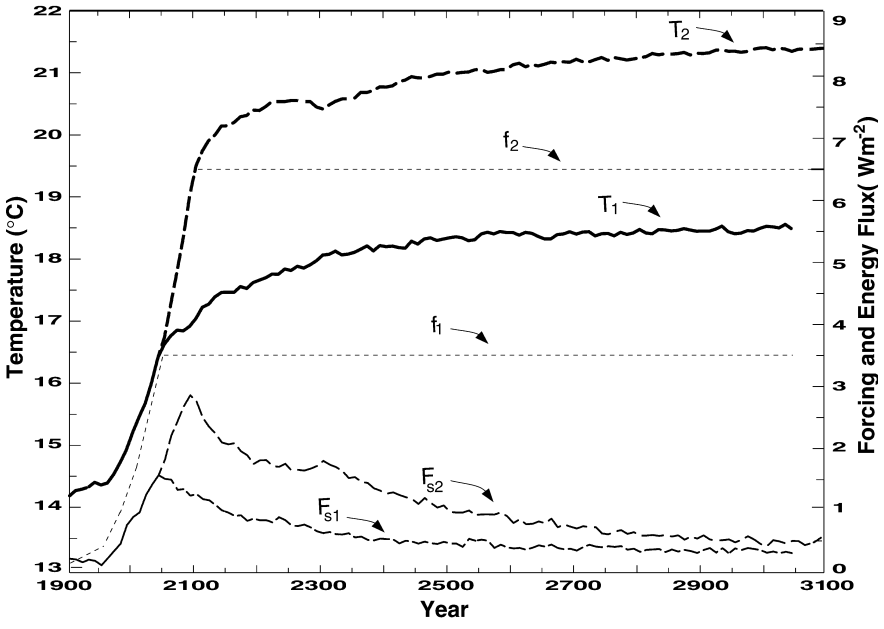

Fig. 1 Global mean radiative forcing $f(\mathrm{Wm}^{-2})$, surface air temperature change $T'(°\mathrm{C})$, and energy flux into the ocean $F_S(\mathrm{Wm}^{-2})$ for simulated climate change following the IS92a greenhouse gas and sulfate aerosol scenario with forcings stabilized at the year 2050 (subscript 1) and year 2100 (subscript 2) values

Figure 1 displays the global mean radiative forcing, global mean surface air temperature change, and energy flux into the ocean for these simulations. The figure shows how the system is committed to a further increase in temperature even after the forcing has been fixed at a constant value. It also shows the very long time scales involved in the adjustment to the new constant forcing level. The long time scales are associated with oceanic adjustment as indicated by the slow reduction of the flux of energy into the oceans as the system approaches a new equilibrium.

4 Radiative forcing and temperature response patterns

According to IPCC (2001), Chapter 6, the term "radiative forcing... denotes an externally imposed perturbation in the radiative energy budget of the Earth's climate system". Figure 2 displays the radiative forcings due to projected GHG and sulfate aerosol increases for the year 2050 together with the resulting surface temperature response patterns averaged over the 2040–2060 period. The results are from the transient climate change simulations described in Boer et al. (2000a,b) following the IS92a forcing scenario. Radiative forcing and temperature differences are calculated with respect to the control simulation of the model representing preindustrial conditions.

The positive GHG forcing pattern f_g, befitting the assumption of well mixed GHGs, is geographically smooth. The negative aerosol forcing pattern f_a is much more localized. The associated temperature response patterns do not much resemble the forcing patterns and it is visually striking that the temperature response pattern T'_a associated with the aerosol forcing more nearly resembles the negative of the distributed GHG response pattern T'_g than the aerosol forcing pattern f_a itself. The relationship between the patterns, in terms of the percentage of explained variance as measured by the square of the spatial correlation, is given in Table 1 for this period and for the 2080–2100 period at the end of the century.

It is notable that the pattern of GHG forcing f_g explains *none* of the resulting temperature change pattern T'_g in the transient climate change calculation, at least as measured by the spatial correlation coefficient (the forcing and response patterns are formally orthogonal to one another under global averaging). The more spatially restricted aerosol forcing pattern f_a is somewhat more successful in explaining (in this statistical way) the associated temperature pattern T'_a, although it accounts for only about 20% of the variance. The more striking result is that the GHG temperature response pattern T'_g explains a comparatively large fraction, 60–66%, of the variance of the aerosol temperature response pattern T'_a, despite a common variance between the forcing patterns f_g and f_a of only 8%. In other words, the temperature response patterns are at best a weak reflection of their parent forcing patterns. Moreover, despite the dissimilarity of their parent forcing patterns, the temperature response patterns exhibit a strong family resemblance. Similar results are reported by Reader and Boer (1998), IPCC (2001) (Sect. 12.2.3), and Forster et al. (2000), among others.

Figure 2 and Table 1 provide some evidence of a "generic" geographical temperature response pattern, say $\mathscr{T}(\lambda, \varphi)$, that depends on the magnitude $\langle f \rangle$ but not the pattern of $f(\lambda, \varphi)$. In this case the GHG response pattern $T'_g \approx \langle f_g \rangle \mathscr{T}$, and the aerosol response pattern $T'_a \approx \langle f_a \rangle \mathscr{T}$ would be similar but opposite in sign since $\langle f_a \rangle$ is negative and the patterns would be additive with $T'_{g+a} \approx \langle f_a + f_g \rangle \mathscr{T}$.

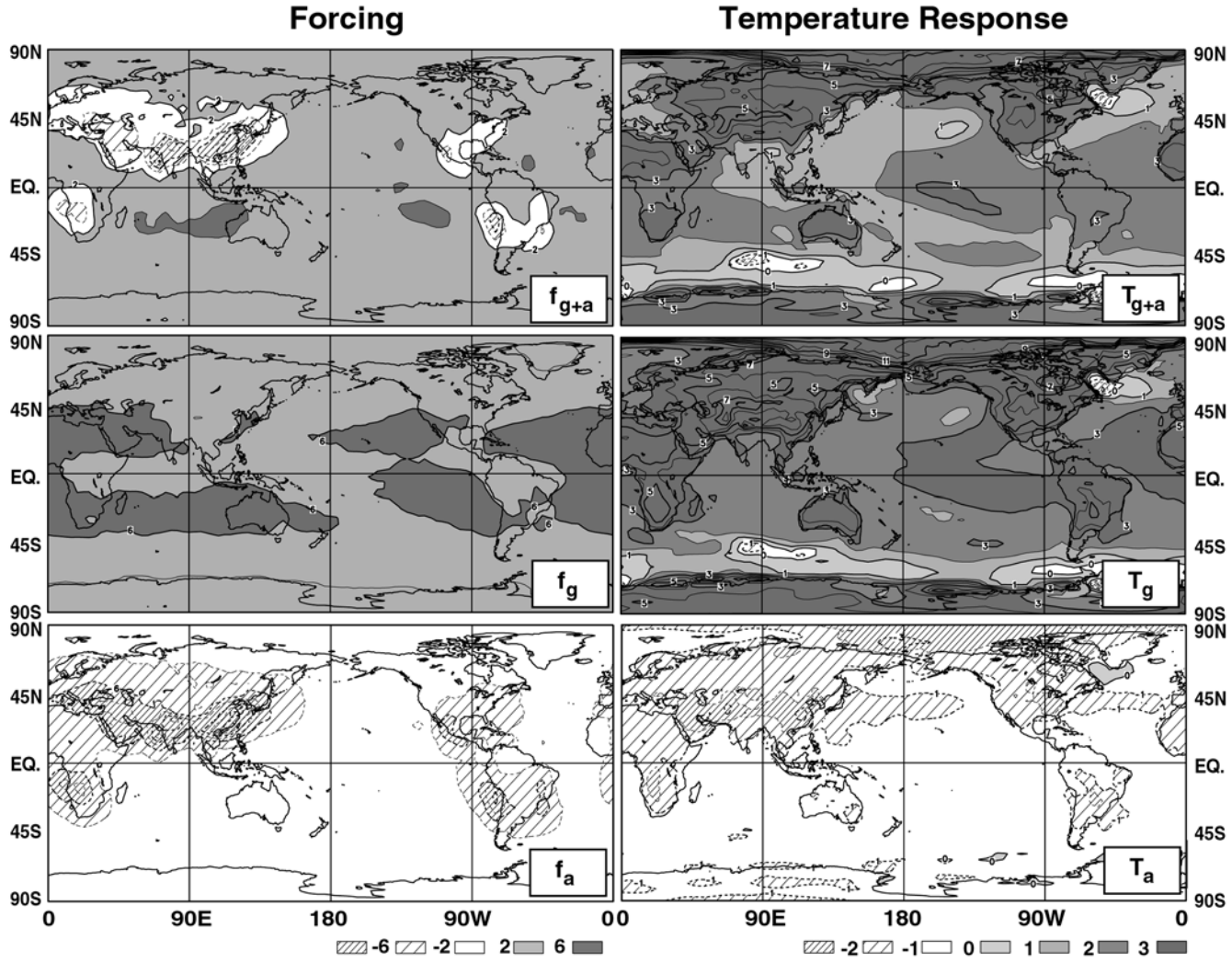

Fig. 2 The geographical distribution of the GHG plus aerosol forcing f_{g+a}, the GHG-only forcing f_g, and the aerosol forcing f_a, at year 2050 (*left panels*) and their associated temperature response patterns averaged over the period 2040–2060 (*right panels*). Units are Wm^{-2}, and °C respectively

Table 1 Global mean forcing (Wm^{-2}) and temperature responses (°C) and the percentage of explained variance relating temperature and forcing patterns measured by the squared spatial correlation coefficient. Values above the diagonal are for the 2040–2060 period and those below for the 2080–2100 period

	T'_g	T'_a	f_g	f_a
Mean 2040–2060	3.3	–0.9	5.5	–2.1
Mean 2080–2100	5.8	–1.3	8.6	–2.0
T'_g	r^2	60	0	3
T'_a	66	–	0	23
f_g	0	0	–	8
f_a	3	17	8	–

Related results are shown by Forster et al. (2000) for a range of very different forcing patterns. For instance, if solar or GHG forcing is confined to the Northern or Southern Hemisphere only, and set to zero in the other hemisphere, the resulting temperature change patterns T'_N and T'_S add to a remarkable degree to give the pattern $T'_G = T'_N + T'_S$ obtained with forcing over the globe. In this case, however, the additivity of the response pattern does *not* imply a generic response pattern. Rather, $T'_N \neq \langle f_N \rangle \mathcal{T} \neq f_N \langle \mathcal{T} \rangle \neq f_N \mathcal{T}$, and the temperature response pattern resembles neither a generic response pattern, the forcing pattern, nor the product of the two, but falls somewhere in between.

In both cases, the linearity (or "additivity") of the temperature response to different amplitudes and patterns of forcing is notable. That is if T'_i is the response to forcing f_i, then also the sum of the response patterns $T' = \sum T'_i$ is the result of forcing the system with the sum $f = \sum f_i$ of the forcing patterns. We investigate the connection between forcing and response in terms of the energy balance of the climate system in what follows.

5 The energy balance of the climate system

The energy balance of the climate system, integrated in the vertical, is written as $dh/dt = A + R$ where A is

the convergence of the horizontal energy flux in the atmosphere and ocean, and R is the net flux of energy into the column at the top of the atmosphere (TOA). Here $\mathrm{d}h/\mathrm{d}t$ is the storage of energy in the column which is dominated by storage in the ocean. The evolving *change* in the energy balance of the climate system due to an external forcing change is written as

$$\frac{\mathrm{d}}{\mathrm{d}t}h' = A' + R' \tag{2}$$

where $X' = X - X_\mathrm{o}$ and primes indicate the change from the unperturbed climate state (indicated by the subscript o).

The radiative perturbation $R' = R - R_\mathrm{o} = (R - R_*) + (R_* - R_\mathrm{o})$ is decomposed into two terms, the *radiative forcing*

$$f = R_* - R_\mathrm{o} \tag{3}$$

representing the externally imposed perturbation to the radiative energy budget of the system and the *radiative feedback*

$$R - R_* = -\lambda T' \tag{4}$$

representing the internally generated radiative response to the change in forcing expressed as a linear function of surface air temperature. The energy budget equation, where all terms, including λ, are functions of *location* and *time*, may be written in several forms as

$$\frac{\mathrm{d}}{\mathrm{d}t}h' = A' + R' = A' + (R - R_*) + (R_* - R_\mathrm{o}) = A' - \lambda T' + f. \tag{5}$$

5.1 Radiative forcing

The concept of radiative forcing is reviewed in Chapter 6 of IPCC (2001). In particular "the radiative forcing of the surface-troposphere system due to the perturbation in or the introduction of an agent ... is the change in the net irradiance ... at the tropopause after allowing for stratospheric temperatures to readjust to radiative equilibrium but with surface and tropospheric temperatures and state held fixed at the unperturbed values". Symbolically

$$R_\mathrm{o} = R(\underset{\sim}{T}_\mathrm{o}, q_\mathrm{o}, c_\mathrm{o}, \ldots;\ g_\mathrm{o}, a_\mathrm{o}, \ldots)$$

is the radiative flux for the unperturbed climate state (indicated by the subscript o) as a function of temperature, moisture, cloud, and any other internal parameters that affect radiation, together with the external parameters such as GHG concentrations and aerosol loadings (symbolically g, a) etc. All symbols in the expression for R represent three-dimensional distributions of the quantities but, since surface temperatures play a special role in sensitivity analysis, the three dimensional distribution of temperature is written as $\underset{\sim}{T}$ to distinguish it from T which is used to represent surface temperature. The perturbation due to the change in the external parameters, but keeping internal variables fixed is

$$R_* = R(\underset{\sim}{T}_\mathrm{o}, q_\mathrm{o}, c_\mathrm{o}, \ldots; g_\mathrm{o} + g', a_\mathrm{o} + a', \ldots)$$

so that the "instantaneous" radiative forcing is

$$f = R_* - R_\mathrm{o} \approx \left(\frac{\partial R}{\partial g}\right)_\mathrm{o} g' + \left(\frac{\partial R}{\partial a}\right)_\mathrm{o} a' + \ldots \tag{6}$$

giving the differential radiative change due to a change of GHG concentrations and aerosol loadings but with the remaining variables retaining their unperturbed values. Following the IPCC definition, the radiative forcing that is connected to the surface temperature via Eq. (1) is to be calculated from the differences in fluxes across the tropopause.

The radiative change at the tropopause calculated from Eq. (6) is termed the "instantaneous radiative forcing" and this is the forcing estimate used in this study and displayed in Figs. 1 and 2. The forcing for various values of GHG concentrations and aerosol loadings are obtained by reintegrating the control simulation for a year during which parallel diagnostic radiative calculations of R_* are performed. The averaged results are used to obtain f_g and f_a.

The "adjusted" radiative forcing, where radiative calculations are made after allowing the stratosphere to come into a new radiative equilibrium but with substratospheric quantities unadjusted, is the version of the radiative forcing favoured by the IPCC. The difference between the instantaneous and adjusted radiative forcing is of the order of 6% according to Shine et al. (1995) for a doubling of CO_2 concentration in the atmosphere. Such a difference is not material for our analysis and we will refer to our estimate of the radiative forcing at/near the tropopause simply as the "forcing" in what follows.

The radiative forcing is estimated at 50 year intervals, namely for the years 1900, 1950, 2000, 2050, and 2100 following the widely used IS92a scenario and as described in Boer et al. (2000a, Sect. 3.1). In particular, changes in GHG concentrations are represented as changes in equivalent CO_2 concentration, and the direct effect of sulphate aerosols by changes in surface albedo associated with prescribed aerosol loading patterns.

5.2 Radiative feedback

Equation (4) serves to define the feedback parameter λ, a function of location and time, as

$$-\lambda T' = R - R_* \approx \left\{ \left(\frac{\partial R}{\partial \underset{\sim}{T}}\right)_\mathrm{o} \left(\frac{\partial}{\partial T}\underset{\sim}{T}\right) + \left(\frac{\partial R}{\partial q}\right)_\mathrm{o} \left(\frac{\partial q}{\partial T}\right) + \left(\frac{\partial R}{\partial C}\right)_\mathrm{o} \left(\frac{\partial C}{\partial T}\right) \right\} T' + \ldots \tag{7}$$

The expression in braces in Eq. (7) indicates symbolically how changes in the radiative fluxes can be related (to first order) to changes in the internal variables of the system and the surface temperature. Here we evaluate the geographical pattern of λ from $R - R_*$ and decompose it into various components but do not explicitly perform the decomposition implied by the terms in the braces (as is done, but in a globally averaged context, by Wetherald and Manabe (1988) for example and extended to second order by Colman et al. (1997)).

6 Climate sensitivity

6.1 Equilibrium climate sensitivity

The *equilibrium climate sensitivity* measures the global mean surface air temperature change for a doubling of CO_2 concentration in the atmosphere after the system has come to a new equilibrium. Under these circumstances $\mathrm{d}\langle h'\rangle/\mathrm{d}t = \langle A'\rangle = 0$ and we recover Eq. (1) from Eq. (5) in the form

$$\langle T'\rangle_{2x} = \langle f\rangle_{2x}/\hat{\lambda}_{2x} = \hat{s}_{2x}\langle f\rangle_{2x} \tag{8}$$

where $\hat{\lambda} = \langle \lambda T'\rangle/\langle T'\rangle$ indicates the temperature weighted global average of the local feedback parameter. Here $\hat{s}_{2x} = \langle T'\rangle_{2x}/\langle f\rangle_{2x}$ is the *equilibrium climate sensitivity parameter* giving the temperature change per unit radiative forcing change ($^\circ\mathrm{C/Wm^{-2}}$) for a doubling of CO_2.

While the equilibrium change in surface air temperature $\langle T'\rangle_{2x}$ is generally itself termed the *climate sensitivity* (IPCC 2001) this is a misnomer since similar relationships could be written for other climate statistics (as is often done for the percentage change in precipitation, for instance, termed the hydrological sensitivity in Boer 1993 and IPCC 2001).

There is a considerable scatter in the equilibrium climate sensitivities of current climate models (IPCC 2001, Fig. 9.18) and, by implication, in our knowledge and understanding of the basic response of the climate system to a change in forcing. Nevertheless, for a given model the value of the feedback/sensitivity parameter is comparatively independent of the nature and pattern of the forcing change. This insensitivity of the global sensitivity, so to say, is investigated at some depth in recent results by Chen and Ramaswamy (1996a,b), Hansen et al. (1997), and Forster et al. (2000) and holds remarkably well considering the range of processes occurring in the (modelled) climate system. There are circumstances where it holds less well, however, i.e. for certain forcings associated with ozone changes and for forcing confined to certain model layers. The general robustness of the proportionality between temperature response climate forcing under most circumstances, as well as the reasons for the exceptions to this, are both of interest.

6.2 Effective climate sensitivity

Since the climate system is not expected to attain a new equilibrium at twice the current atmospheric CO_2 concentration, the equilibrium climate sensitivity is basically a modelling concept which cannot be directly applied to the actual climate system. The *effective climate sensitivity* is potentially measurable and is obtainable from the globally averaged version of Eq. (5) in the form (Murphy 1995; IPCC 2001, Chapter 9)

$$\frac{\mathrm{d}}{\mathrm{d}t}\langle h'\rangle = -\hat{\lambda}\langle T'\rangle + \langle f\rangle$$

whence diagnostically

$$\hat{\lambda} = 1/\hat{s} = \left(\langle f\rangle - \frac{\mathrm{d}}{\mathrm{d}t}\langle h'\rangle\right)/\langle T'\rangle = -\langle R - R_*\rangle/\langle T'\rangle \ . \tag{9}$$

Nominally, Eq. (9) can be used to estimate the effective climate sensitivity from observations provided that the heat storage term in the ocean and the radiative forcing can be measured or estimated.

It is certainly a broad assumption that the effective sensitivity is comparatively constant for different climate forcing patterns, magnitudes and, in the time dependent case, temporal histories. If the effective climate sensitivity depends importantly on the nature or history of the forcing in a transient calculation then the use of equilibrium climate sensitivity to calibrate simpler models or the consequences of different forcings scenarios will be compromised. Watterson (2000) reports that the climate sensitivity of the CSIRO model is generally stable while there is some evidence that climate sensitivity is a modest function of time and climate state for the Hadley Centre model (Senior and Mitchell 2000) and the CCCma model (Boer and Yu Submitted 2002).

If the climate sensitivity is not effectively constant, the rate of warming for a climate model (or for the climate system) is not completely determined by its equilibrium sensitivity but rather $\langle T'\rangle = \hat{s}(t)\langle f - \mathrm{d}h'/\mathrm{d}t\rangle$ with the terms approaching their equilibrium values as the system does. In this case the transient warming of the system is not necessarily an indication of the equilibrium warming and models with different equilibrium sensitivities may exhibit transient rates of warming that are not proportional to their sensitivities. In fact, for simulations of twentieth century warming based on very similar forcing scenarios, GCMs produce rather similar warmings despite differences in equilibrium sensitivities. This is noted in Boer (2000a, Sect. 4.3) and IPCC (2001) (Chapter 9) and analyzed further in Raper et al. (2002) who argue that differences in the heat storage term tends to compensate for differences in (equilibrium) sensitivity.

Although, the effective climate sensitivity is apparently not entirely constant and equal to its $2 \times CO_2$ equilibrium value, the recent investigations of Chen and Ramaswamy (1996a,b), Hansen et al. (1997) and Forster et al. (2000) suggest that the robustness of the

(approximately) linear relationship between equilibrium global mean temperature response and global mean forcing make both concepts useful in a broad sense.

7 Response to forcing

We explain the forcing/response behaviour (points P1–P3 of the Introduction as discussed and illustrated in Fig. 2 and Table 1) in terms of a feedback/response hypothesis which states that, to first order, temperature response patterns are determined by the geographical pattern of local feedback processes. Robust feedback processes act to "localize" the response both to local and also to remote forcing changes, which are felt locally via system transport processes. The local feedback processes thereby generate a temperature response pattern which depends primarily on the pattern of feedbacks and only secondarily on the pattern of the forcing.

For a system in equilibrium the temperature response pattern from Eq. (5) satisfies

$$T' = (f + A')/\lambda = s(f + A') \ . \tag{10}$$

In the absence of transport changes, A', the temperature response would be determined entirely by the product of the forcing and the local feedback parameter $T' = f/\lambda = sf$. In this case, the temperature response would be zero wherever the forcing was zero, and the product of the sensitivity parameter and the forcing pattern elsewhere. For spatially constant forcing, which is roughly the case for GHG forcing, the temperature response pattern would, in this rather special case, be entirely determined by the local sensitivity parameter s (or equivalently the local feedback parameter λ).

Of course transport changes are not zero and will also respond to forcing changes (e.g. Boer 1995). Nevertheless, Eq. (10) suggests diagnostically how the pattern of local feedback processes, measured by λ, plays an important role in determining the temperature response pattern.

7.1 Local climate sensitivity/feedback

Equation (5) offers the possibility of diagnosing a local feedback parameter from observations or from climate model simulations. Most feedback/sensitivity calculations are performed in the context of a column model or for the global average and so do not explicitly involve transport changes A'. In the energy Eq. (5) there is a separation into local radiative forcing f, local radiative feedback $-\lambda T'$ and the transport change A' which may nominally be termed the local dynamical feedback although, since $\langle A' \rangle = 0$, dynamical feedbacks are only implicit in the globally averaged case.

While the local feedback parameter λ can nominally be diagnosed from Eq. (5), such a calculation is sensitive to error, especially where temperature change is small. Here information on the distribution of local feedback is expressed in terms of the local contribution λ_l to the global feedback parameter $\hat{\lambda}$ where $\hat{\lambda} = \langle \lambda_l \rangle = \langle \lambda T' / \langle T' \rangle \rangle$. From Eq. (5)

$$\langle \lambda T' \rangle = \hat{\lambda} \langle T' \rangle = \langle A' + f - \mathrm{d}h'/\mathrm{d}t \rangle = \langle f - R' \rangle \tag{11}$$

so that

$$\lambda_l = -\Lambda_l = (A' + f - \mathrm{d}h'/\mathrm{d}t)/\langle T' \rangle = (f - R')/\langle T' \rangle \tag{12}$$

gives the *local contribution* to the global feedback parameter.

The geographical distribution of the temperature response and of the local contribution to the feedback parameter are plotted in the upper panels of Fig. 3. The "signed" feedback parameter $\Lambda_l = -\lambda_l$ is plotted since, by definition, positive λ indicates the strength of the *negative* temperature feedback. The sign of Λ_l directly indicates regions of positive or negative feedback. The forcing and transport components of Λ_l are plotted in the lower panel of Fig. 3. The storage term is small and is not plotted. The results apply to the period 500 simulated years after the forcing is stabilized at its year 2050 value in the IS92a scenario, are based on 50-year averages, and are slightly smoothed using a 5-point Shapiro (*1970*) filter. Note that we will subsequently omit the subscript l for the local contribution when the meaning is clear from the context.

The temperature response in Fig. 3 displays a characteristic global warming response pattern with warmest temperatures at high latitudes and over land. The radiative forcing term $f/\langle T' \rangle$ does not, as we have been at pains to stress, resemble the temperature response pattern. Positive regions of the feedback parameter Λ are concentrated over the Arctic Ocean and northern continents, over the extreme southern ocean, and near the date-line in the equatorial Pacific in association with the mean El Nino response simulated in the model (Yu and Boer 2002). Of course on a global basis Λ must be negative to counteract the positive radiative forcing, and the remaining ocean regions and lower latitude land all contribute to a globally negative feedback. High temperature response tends to be largest where Λ is positive although this is not always the case. For instance, while the land generally warms more than the oceans most low latitude land regions nevertheless exhibit negative contributions to Λ.

The geographical distribution of the local feedbacks processes operating in the climate model and measured by Λ are obtained diagnostically and can be regarded as a robust characteristic of the climate model and, in so far as the model reflects reality, of the climate system. From the diagnostic calculation the transport term A' contributes importantly to Λ. This is not to say that transport changes themselves drive the climate response since from Eq. (5) and (12) these transport changes are linked to radiative changes in the climate change simulation as is investigated below.

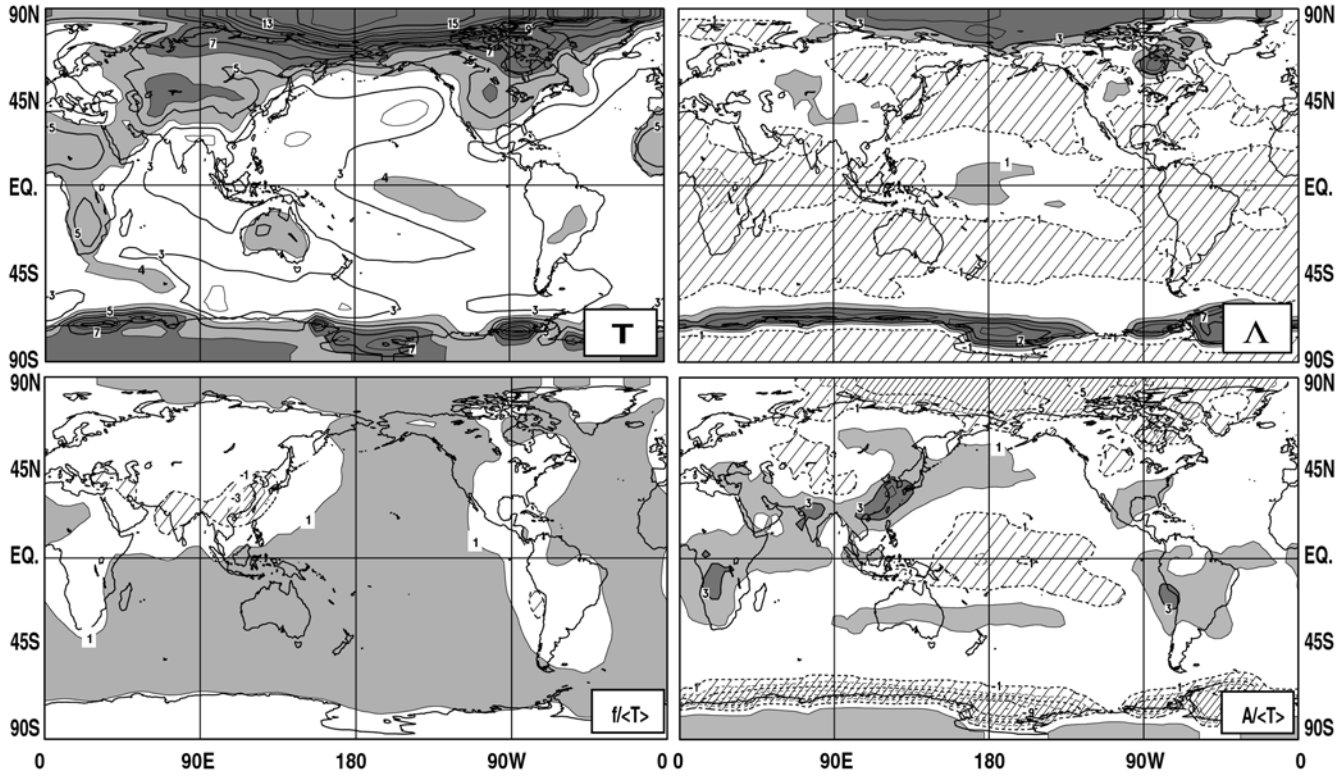

Fig. 3 The geographical distribution of the temperature response T', the local contribution to the global feedback parameter $\Lambda = -\lambda$, and its forcing $f/\langle T' \rangle$ and transport $A'/\langle T' \rangle$ components. Values are 50-year averages for the period 500 years after the forcing is stabilized at its year 2050 value. Units are °C, and Wm^{-2}/°C respectively

7.2 Radiative response processes

Transport changes mediate between forcing and feedback processes and the two are closely related though Eq. (12). The local contribution to the global feedback may also be expressed as

$$\Lambda_l = -\lambda_l = (R' - f)/\langle T' \rangle = ((\tilde{R}' - f) + C)/\langle T' \rangle = \Lambda_A + \Lambda_C$$

where $R' = \tilde{R}' + C$ represents the decomposition of the radiative change R' into cloud-free Atmosphere/surface and Cloud feedbacks. The no-cloud feedback $\tilde{R}'$ is obtained by repeating the radiative calculations setting cloud amounts to zero but with all other quantities remaining the same. The cloud feedback $C = R' - \tilde{R}'$ represents the radiative effects of cloud changes. As discussed in Zhang et al. (1996) for instance, the cloud feedback contribution defined in this way differs somewhat from the component in Eq. (7) involving cloud changes which is also be referred to as cloud feedback in some studies.

The feedback Λ is decomposed into cloud-free atmosphere/surface and cloud-only feedbacks, $\Lambda = \Lambda_A + \Lambda_C$, in the first row of panels in Fig. 4 and into shortwave and longwave components, $\Lambda = \Lambda_S + \Lambda_L$ in the first column of Fig. 4. Each of the terms is further decomposed to give the nine components

$$\Lambda = \Lambda_A + \Lambda_C = \Lambda_S + \Lambda_L = \Lambda_{SA} + \Lambda_{LA} + \Lambda_{SC} + \Lambda_{LC} = \sum \Lambda_i$$

in the remainder of Fig. 4. Table 2 gives the globally averaged value of each of the components $\langle \Lambda_i \rangle$ and their spatial variances $\sigma^2_{\Lambda_i} = \langle \Lambda_i^{+2} \rangle$, as a measure of spatial structure, where Λ^+ is the spatial deviation from the global average. The contributions of the components to the spatial variance from

$$1 = \sum \langle \Lambda^+ \Lambda_i^+ \rangle / \sigma^2_\Lambda = \sum V_i \qquad (13)$$

are also given. The spatial correlations between components $r_{ij} = \langle \Lambda_i{}^+ \Lambda_j{}^+ \rangle / \sigma_{\Lambda_i} \sigma_{\Lambda_j}$ appear in the lower part of the table.

The atmosphere/surface or no-cloud feedbacks Λ_A are the radiative consequences of changes in the distribution of temperature and moisture in the atmosphere and also of changes at the surface but not of changes in cloud distribution or optical properties. The strong positive surface albedo feedback associated with the retreat of snow and sea-ice cover is clearly seen in the shortwave component, Λ_{SA}. The longwave atmosphere-only feedback Λ_{LA} will have contributions from the enhanced blackbody radiation from the warmer surface, a negative feedback, and also as a consequence of change in the temperature and moisture content of the atmosphere. The result for Λ_{LA} is the expected negative feedback with the exception of the region of positive feedback in the tropical central-western Pacific associated with the mean El Nino response to global warming

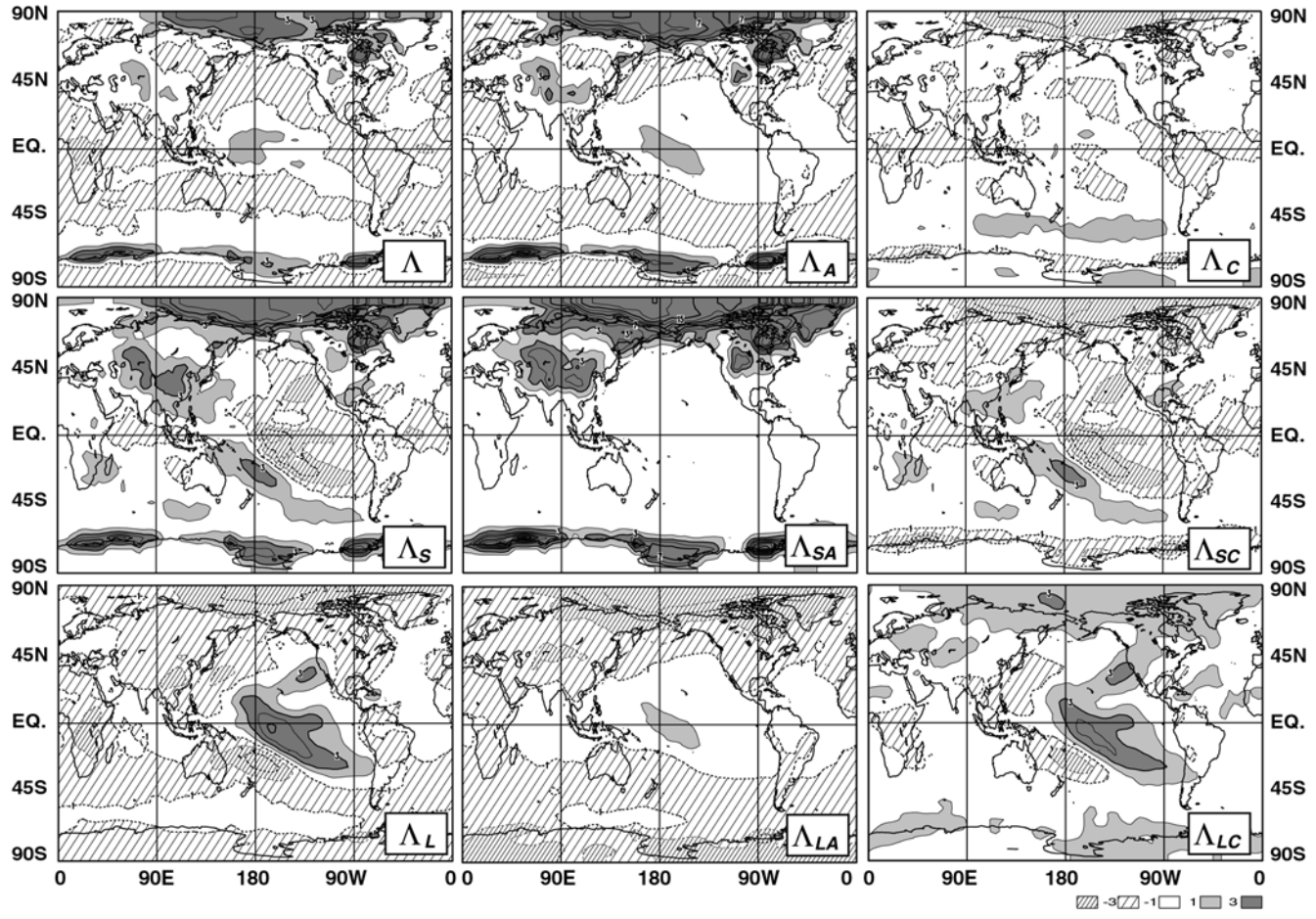

Fig. 4 The decomposition of the local feedback contribution Λ of Fig. 3 into components $\Lambda = \Lambda_A + \Lambda_C = \Lambda_S + \Lambda_L = \Lambda_{SA} + \Lambda_{LA} + \Lambda_{SC} + \Lambda_{LC}$ where A and C indicate cloud-free atmosphere/surface and cloud-only components, and S and L indicate shortwave and longwave components. Units are $Wm^{-2}/°C$

Table 2 Spatial means, variances, correlations, and variance contributions of and between the components of the feedback

	Λ	Λ_S	Λ_L	Λ_A	Λ_C	Λ_{SA}	Λ_{SC}	Λ_{LA}	Λ_{LC}
$\langle\Lambda_i\rangle$	–0.80	0.10	–0.90	–0.38	–0.42	0.95	–0.85	–1.33	0.43
$\sigma_{\Lambda_i}^2 = \langle\Lambda_i^{+2}\rangle$	2.51	5.65	3.60	4.28	1.44	7.72	3.58	1.59	2.02
$V_i = \frac{\langle\Lambda^+\Lambda_i^+\rangle}{\sigma_\Lambda^2}$	1	0.91	0.09	1.07	–0.07	1.34	–0.43	–0.27	0.36
Λ	1	0.61	0.08	0.82	–0.09	0.76	–0.36	–0.34	0.40
Λ_S		1	–0.75	0.54	–0.12	0.74	0.17	–0.76	–0.33
Λ_L			1	0.01	0.08	–0.29	–0.51	0.66	0.75
Λ_A				1	–0.65	0.91	–0.66	–0.35	0.33
Λ_C		Correlations			1	–0.55	0.66	0.16	–0.03
Λ_{SA}						1	–0.54	–0.72	0.25
Λ_{SC}							1	0.11	–0.77

in the model. Table 2 nevertheless shows that the overall cloud-free atmosphere/surface feedback $\langle\Lambda_A\rangle$ is negative.

The cloud feedback Λ_C displays a comparatively flat pattern which is largely negative but which has modest regions of positive feedback also. According to Table 2, the clear-sky atmosphere/surface and cloud feedbacks each contribute about half to the overall feedback of the model in the global mean. The shortwave cloud feedback Λ_{SC} of the mean El Nino response is clearly seen in the Pacific with increased and optically thicker clouds in the central east Pacific providing negative Λ_{SC} while decreased cloud amounts in a "horse shoe" in the western Pacific provide positive feedback. The characteristics of the cloud feedbacks associated with the El Nino response are consistent with the cloud-albedo mechanisms (e.g. Ramanathan and Collins 1991; Meehl and Washington 1996) which highlight the increase in cloud shielding and the reduction of solar radiation at the surface associated with enhanced convection. The

signature of the mean El Nino response in the model is discussed in detail in Yu and Boer (2002).

The geographical structure of the feedback pattern Λ arises as the sum of the various component feedbacks. The visual impression from Fig. 4 is that the structure of the feedback pattern Λ is largely that of the cloud free atmosphere/surface Λ_A and this is confirmed by the large correlation between the two patterns ($r = 0.82$) which is in turn influenced strongly by the solar clear-sky component Λ_{SA} ($r = 0.76$). The cloud feedback pattern Λ_C is almost uncorrelated ($r = -0.09$) with Λ but strongly negatively correlated ($r = -0.65$) with the clear sky feedback Λ_A and so counteracts it. The solar Λ_S and longwave Λ_L feedbacks oppose one another ($r = -0.75$) as do solar and longwave cloud feedbacks ($r = -0.77$).

One way of quantifying the contribution of the various components to the geographical structure (rather than the mean) of Λ is by way of Eq. (13). According to Table 2, the solar contribution V_S dominates over the longwave contribution V_L, and the clear sky V_A over cloud feedback V_C which contributes negatively but weakly to Λ. The contributions from the subcomponents indicate that the V_{SA} contribution dominates, that V_{LC} contributes less importantly while V_{SC} and V_{LA} contribute negatively. The components contribute to the spatial structure of the feedback, as measured by the spatial variance, somewhat differently than they contribute to the mean although the sense of the contributions are the same throughout. There is a certain symmetry with Λ_{SA} and Λ_{LC} positively correlated with Λ and contributing positively to the mean and the spatial variance while Λ_{SC} and Λ_{LA} are negatively correlated with Λ and contribute negatively to the mean and the spatial variance. This broadly indicates some of the physical processes at play, at least in this model.

The interpretation of the decomposition as representing processes which determine the distribution of the local feedbacks measured by Λ depends, of course on what is considered to constitute a process. In some analyses (e.g. Hansen et al. 1984; Wetherald and Manabe 1988; Zhang et al. 1996) and corresponding to the bracketed expression in Eq. (7), the radiative changes are decomposed into changes associated with the change in the amount and distribution of moisture, the lapse rate, and so on. Here we examine the contribution to the global feedback of changes in the basic radiative components which are, in turn, linked to changes in temperature, cloudiness, and surface albedo. It would require additional steps to ascribe the changes further and we do not attempt this here.

All the feedback components, with the exception of Λ_{SA}, display regions of both positive and negative values. The mechanisms determining Λ vary over land and ocean, at high latitudes and low, and generally from place to place. The decomposition of feedback processes into various components does not provide a physical picture that operates everywhere but rather there is a superposition of processes that themselves vary with location so that the result is dominated by different processes in different regions (at least in the kind of decomposition represented by Fig. 4). The interrelated processes nevertheless produce a robust pattern of feedback characterizing the response to climate forcing.

7.3 Zonally averaged budget terms

The zonally averaged versions of the terms in Eqs. (11–12) for the GCM paralleling Fig. 3 are displayed in the left hand panels of Fig. 5. The forcing f is roughly constant with latitude but the temperature response T' varies with latitude, most strongly at high latitudes. Note that the feedback parameter Λ varies relatively smoothly with latitude but also that it changes sign; negative feedback is found over much of the globe but positive feedback is found at high latitudes. The transport term A' also varies relatively smoothly with latitude and $f + A'$ varies roughly as $\lambda = -\Lambda$. The storage term is small, since the system is approaching equilibrium, and is not plotted.

8 An illustrative model of climate feedback/response

We appeal to the zonally averaged energy budget quantities in Fig. 5 to develop an illustrative model (IM) which is consistent with points (P1–P3) of the Introduction and which supports the climate feedback/response hypothesis. Although the illustrative model is developed in the zonal context the arguments are meant to apply also to the geographically distributed case.

The equilibrium zonally averaged version of Eq. (5) is written as

$$A'(\varphi) - \lambda(\varphi)T'(\varphi) + f(\varphi) = 0 \qquad (14)$$

where the dependence of all terms on latitude is explicitly noted. The radiative forcing term $f(\varphi)$ results from changes to external parameters and is known. The feedback parameter $\Lambda(\varphi) = -\lambda(\varphi)$ is taken to be a known feature of the climate system and is specified based on the diagnostic analysis of GCM results in Fig. 5.

Equation (14) may be solved for the temperature distribution provided the transport term can be expressed as a function of temperature $A' = A(T'(\varphi))$. A simple representation that has been used in the climate context (e.g. Stocker et al. 1992 and references therein) relates the transport linearly to the meridional temperature gradient. With this approximation Eq. (14) becomes

$$\frac{\kappa}{a^2 \cos\varphi}\frac{\partial}{\partial\varphi}\cos\varphi\frac{\partial}{\partial\varphi}T' + \Lambda(\varphi)T'(\varphi) + f(\varphi) = 0 \qquad (15)$$

which may be solved with no-flux boundary conditions at the poles.

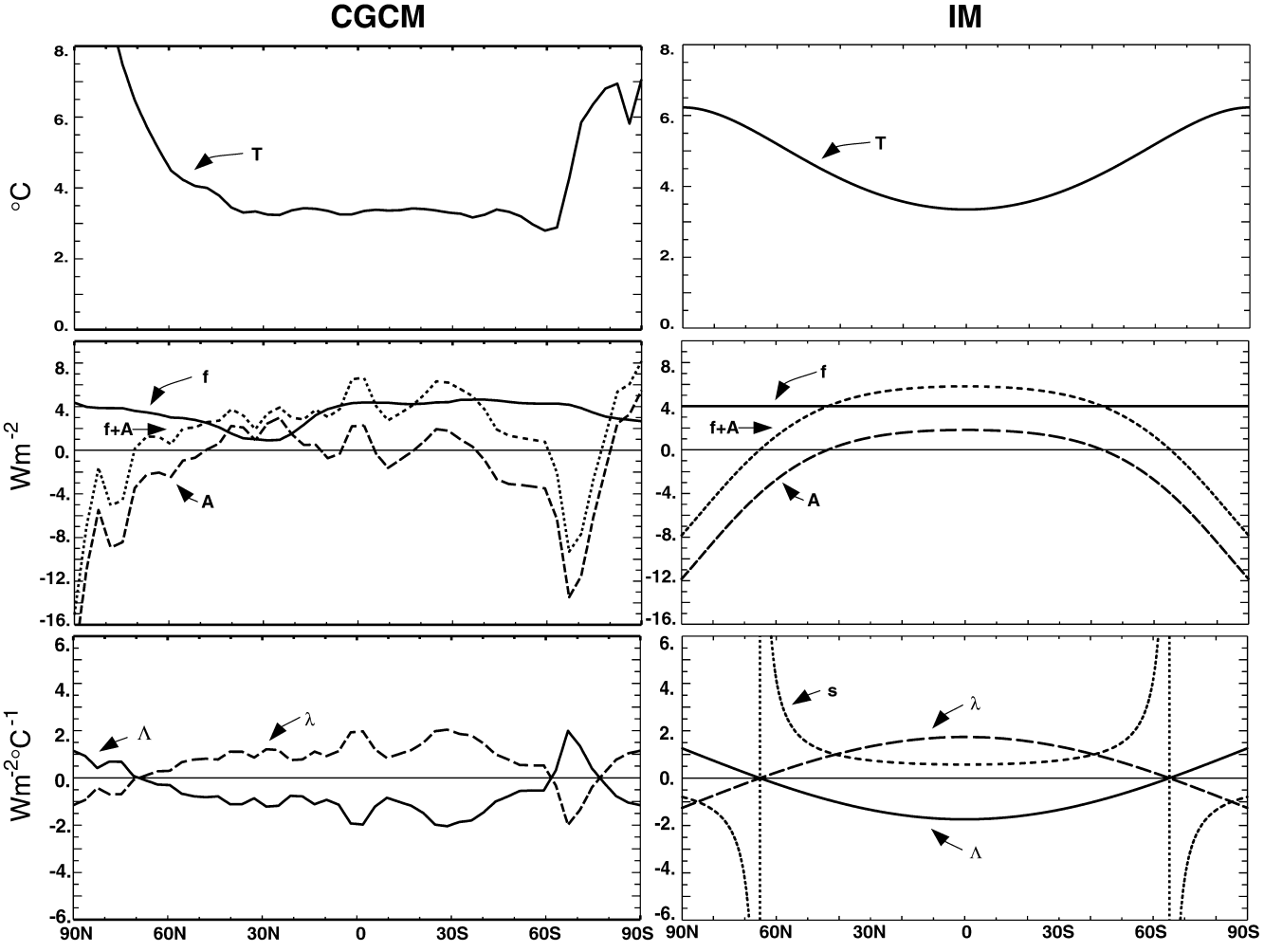

Fig. 5 Zonally averaged temperature response T'(°C), forcing f, transport change A' (Wm^{-2}), and feedback parameters $\Lambda = -\lambda(Wm^{-2}/°C)$. Results from the GCM, paralleling Fig. 3, are plotted in the *left hand panels* and those from the illustrative model with specified forcing $f = 4\ Wm^{-2}$ and climate sensitivity parameter $\Lambda = -\lambda = -1/s = 3.0\ (\cos(\varphi) - 0.42)\ Wm^{-2}/°C$ are plotted in the *right hand column*

The feedback parameter is represented as $\Lambda = -\alpha(\cos(\varphi) - \beta)$ with $\alpha = 3.0\ Wm^{-2}/°C$, and $\beta = 0.42$, (giving the boundary of the positive and negative feedback regions near 65° north and south) based on the distribution from the GCM. A reasonable value of the parameter κ, which implicitly includes factors that arise in the vertical integration of the energy budget, is $\kappa/a^2 = 0.5\ W/°C$ (Stocker et al. 1992). Results are not strongly dependent on these choices (not shown). The solution of Eq. (15) for constant forcing $f = 4\ Wm^{-2}$ is shown in the right hand panels of Fig. 5 and is a smoothed and idealized version of the GCM results but with similar magnitudes and features.

The result may be interpreted in a stepwise fashion: the constant forcing acts to warm the system everywhere, the resulting temperature increase is acted on differentially by the feedback processes represented by Λ which amplify the warming in the polar regions of positive feedback and counteract it in lower latitude regions of negative feedback. Transport change operates to smooth out this temperature pattern by differentially transporting energy equatorward, that is, from regions of positive (or weaker negative) feedback to regions of (larger) negative feedback. The differential transport change represents a decrease in the usual equator to pole transport in this case. The resulting temperature structure is the balance between these competing processes and is critically dependent on the structure and magnitude of the feedback parameter. The distribution of feedback processes, represented by Λ, is considered, in this view, to be a basic feature of the climate system and a determinant of the geographical distribution of the temperature response.

8.1 Response to different forcing patterns

The illustrative model can explain the kinds of results obtained in Fig. 2 where the temperature response is a ''characteristic'' pattern even though the forcing has

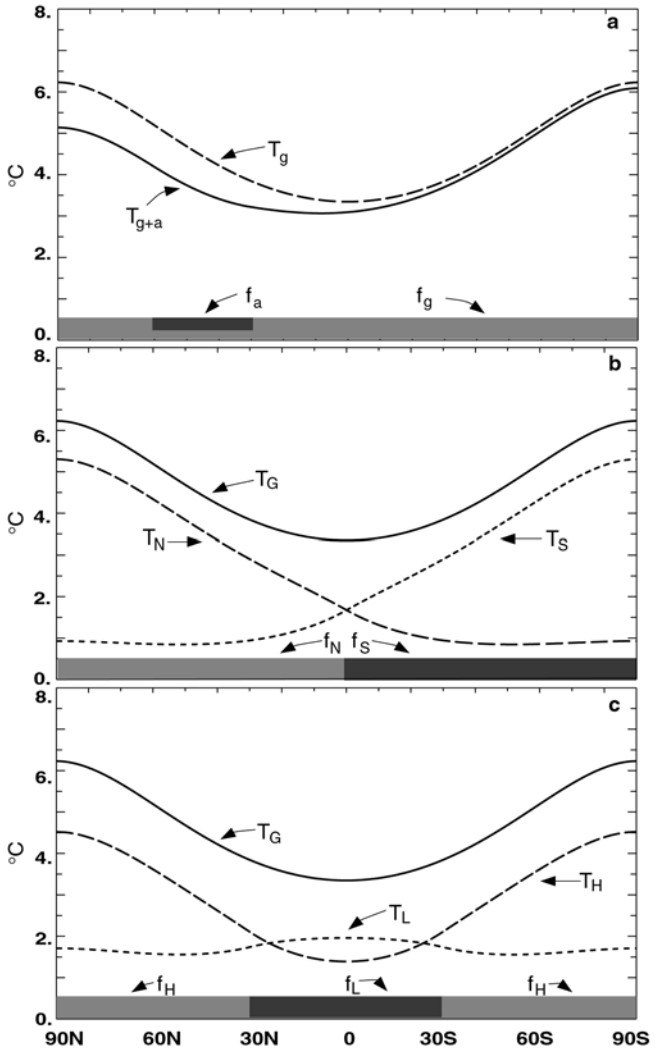

Fig. 6 Temperature response patterns T'(°C) from the illustrative model with the specified climate sensitivity parameter $\Lambda = 3.0(\cos(\varphi) - 0.42)$ $Wm^{-2}/°C$ of Fig. 5 and for forcing distributions illustrated by the *shaded bands* in the *panels*. *Upper panel*, the temperature response T'_g for a geographically constant GHG-like forcing $f_g = 4$ Wm^{-2} (*light shading*) and for a GHG + aerosol-like forcing case T'_{g+a} where the negative aerosol forcing $f_a = -2$ Wm^{-2} (*dark shading*) reduces the net forcing in a localized latitude band. *Middle panel*, temperature response T'_G to uniform forcing f_G over the globe and seperately, T'_N and T'_S for forcing confined to the Northern f_N and Southern f_S Hemispheres only. *Bottom panel*, temperature responses T'_L and T'_H for forcing f_L confined to tropical low latitudes between 30° north and south, and seperately for forcing f_H at extratropical high latitudes

local structure. This is illustrated in the upper panel of Fig. 6 where comparatively localized negative aerosol forcing f_a is superimposed on a broad positive GHG forcing f_g as indicated by the shaded band. The response T'_g to geographically constant forcing f_g is indicated by the dashed line while the response to the combined forcing $f_g + f_a$ is the solid line T'_{g+a}. The magnitude of the warming has been reduced but the pattern is similar in the two cases. The localized negative aerosol forcing has not introduced a local decrease in the temperature response and the largest effect is seen at the pole. The negative feedback operating at the forcing latitude together with the dispersion of the forcing by the transport change gives a result which resembles that of the case with constant forcing. This is the kind of response seen where the comparatively localized negative aerosol forcing is added to the broadly distributed positive GHG forcing in Fig. 2.

The results obtained for much more dramatic forcing structures can also be illustrated as can the additivity of temperature response patterns. Forster et al. (2000) use a GCM to investigate a range of sensitivity questions. They note particularly the additivity of temperature response patterns and the general, although not complete, stability of the global mean climate sensitivity to an array of forcing types and patterns. Although we are unaware of the structure of the feedback parameter for that model we are able to reproduce its behaviour qualitatively using a feedback parameter based on that of the CCCma model in Fig. 5. The middle panel of Fig. 6 displays the results obtained in the special cases of constant forcing for the globe and separately for the northern and southern hemispheres only. The response patterns closely resemble those of Forster et al. (2000, Fig. 9), obtained with their GCM for these rather extreme forcing cases both in the distribution of the temperature response and in the additivity of the result.

The case for global, low, and high latitude forcing is shown in the bottom panel of Fig. 6 which again reproduces the Forster et al. (2000) results for that case. For tropical forcing there is nevertheless an appreciable temperature response in the extratropics, even though there is no forcing there. The change in the transport of energy from the tropics to higher latitudes allows the positive feedbacks there to operate to give an appreciable temperature response in the absence of local forcing.

8.2 Role of dynamics

The feedback/response hypothesis is characterized by the geographic distribution and robustness of Λ and its first order independence of the climate state. The feedbacks "localize" the response to forcing, even to forcing that is remote. The climate change pattern tends to be generic and determined by the distribution of the feedbacks while the transport changes are a reactive intermediary between forcing and feedback. In this view, local feedback processes are critical and dynamical changes are secondary and this differs, for instance, from the non-linear dynamical perspective (e.g. Palmer 1999) which postulates that the response is determined by the non-linear dynamics of the system as affected by small amplitude changes in forcing.

9 Additivity and sensitivity

The additivity of temperature response patterns follows straightforwardly from the feedback/response hypothe-

sis. It also follows, however, that the independence of the global sensitivity to the pattern of the forcing is only approximate.

9.1 The additivity of temperature patterns

If T'_i is the response to forcing f_i, the additivity of temperature response patterns requires that $T' = \Sigma T'_i$ be the response to the sum of the forcings $f = \Sigma f_i$. This follows directly by summation of Eq. (10) in the form

$$A(T'_i) - \lambda T'_i + f_i = 0, \tag{16}$$

provided that A is a linear function of T', i.e. that $\Sigma A(T'_i) = A(\Sigma T'_i) = A(T')$. The additivity of temperature response patterns depends on the feedback parameter λ being reasonably independent of the temperature response and the transport change term being a reasonably linear function of temperature response. Of course this cannot be the case for any and all perturbations to the climate system but the reasonably broad range of cases for which it applies, at least in the context of GCMs, attests to its first order robustness.

9.2 The constancy of climate sensitivity

The proportionality between globally averaged forcing and globally averaged temperature change is measured by the climate sensitivity parameter $\hat{s}$ as expressed in Eq. (1). The utility of the climate sensitivity resides in its comparative independence of the nature and pattern of the forcing and in the additivity of the results. To the extent that Eq. (1) holds, the global mean temperature change follows when the global mean forcing is known. Experimentally, this behaviour appears to be reasonably robust in climate models although there are certain exceptions (e.g. Hansen et al. 1997).

The form of Eq. (16), however, implies that Eq. (1) holds only approximately and climate sensitivity is generally *not* constant and independent of forcing pattern and magnitude but only approximately so. The constancy of the *local* sensitivity parameter λ implies that $\hat{s}$ or $\hat{\lambda}$, which measure the sensitivity for global averages, are not independent of the forcing. Thus for λ a prescribed function of location, $\langle \lambda T'_i \rangle = \hat{\lambda}_i \langle T'_i \rangle = \langle f_i \rangle$ implies that

$$\hat{s}_i = \langle T'_i \rangle / \langle \lambda T'_i \rangle$$

depends on the temperature response pattern T'_i which differs for different forcing patterns f_i. The linear relationship between globally averaged forcing and temperature response embodied in Eq. (1) is only approximate.

If the spatial gradients of the forcing are not too large, the response tends toward a generic response as illustrated in Figs. 2 and 6a and represented as $T'_i \approx \langle f_i \rangle \mathscr{T}$ for $\mathscr{T}$ the generic geographical temperature response pattern. In this case

$$\hat{\lambda}_i = \langle \lambda T'_i \rangle / \langle T'_i \rangle \approx \langle \lambda \langle f_i \rangle \mathscr{T} \rangle / \langle \langle f_i \rangle \mathscr{T} \rangle = \langle \lambda \mathscr{T} \rangle / \langle \mathscr{T} \rangle = \hat{\lambda}$$

and $\hat{\lambda}$ will be constant and independent of the forcing to the extent that the response pattern is generic.

It is intuitively obvious, and also follows from Eq. (16) and the expression for $\hat{s}$, that forcing the system preferentially in a region of positive feedback will result in a larger response than forcing the system preferentially in a region of negative feedback. This will translate also into a larger global sensitivity even if the global average forcing is the same in the two cases. Both the comparative stability of $\hat{\lambda}$ but also this dependence on forcing location is seen in the illustrative model as well as in GCMs.

Sensitivity results for models consisting of an atmospheric GCM coupled to mixed layer ocean component are available for a range of forcings in Hansen et al. (1997, Table 4, column 5) and Forster et al. (2000, Tables 1 and 2). Table 3 compare some results from the mixed layer version of the CCCma model, the Forster et al. (2000) model, and the illustrative model (IM) of Sect. 8. Note that the climate sensitivity of this version of the CCCma model is close to twice that of the Forster et al. (2000) model for the standard $2 \times CO_2$ experiment (and by construction for the IM). Results are very consistent when this factor of 2 is applied.

Table 3 indicates the stability of $\hat{s}$ for a range of quite different forcings, in the Forster et al. (2000) model and in the IM including different magnitudes (4 and 6 Wm^{-2}) and patterns (NH and SH) of forcing. For the IM it follows from Eq. (15) that the sensitivity will be constant and the temperature changes strictly additive if the forcing f is symmetric with respect to the specified (symmetric) feedback parameter $\Lambda = -\lambda$. The Forster et al. (2000) model also displays this kind of behaviour

Table 3 Dependence of the global sensitivity parameter $\hat{s}$ (°C/Wm^{-2}) on the magnitude and distribution of the forcing f. Results compare the illustrative model (IM) with the Forster et al. (2000) results (their Table 2). The bottom two rows give the equilibrium $2 \times CO_2$ climate sensitivity from the Forster et al. model and the mixed layer ocean version of the CCCma coupled model. Note that the $2 \times CO_2$ sensitivity for the CCCma model and, by construction, the IM is very close to a factor of two larger than that of the Forster et al. model. The results for $\langle T' \rangle$ and $\hat{s}$ agree closely for the different forcing distributions after scaling with this factor

Spatial distribution of forcing f	IM			Forster		
	$\langle f \rangle$	$\langle T' \rangle$	$\hat{s}$	$\langle f \rangle$	$\langle T' \rangle$	$\hat{s}$
Global	4.0	4.1	1.03	3.7	1.7	0.47
Global	6.0	6.2	1.03	5.9	2.7	0.46
SH only	3.0	3.1	1.03	2.9	1.4	0.47
NH only	3.0	3.1	1.03	3.0	1.3	0.45
30°N–30°S only	3.0	2.6	0.88	3.0	1.1	0.37
Extratropics	3.0	3.6	1.19	2.9	1.6	0.55
$2 \times CO_2$/Forster		1.74	0.47			
$2 \times CO_2$/CCCma		3.50	1.09			

which indirectly argues for the symmetry of the feedback parameter in that model.

The coherence between the GCM results and those of the IM extend also the case of tropical and extratropical forcing (provided the factor of 2 in sensitivity is kept in mind). In both cases, forcing in the tropical region (of negative feedback) results in a smaller temperature change and value of the sensitivity parameter than does the equivalent amount of forcing in the extratropical region (of at least partial positive feedback).

Although the IM is very simple it is able to reproduce results from an independent GCM, at least latitudinally and qualitatively, based on the distribution of the feedback parameter obtained diagnostically from the results of the CCCma fully coupled model (i.e. an AGCM coupled to a full OGCM). The apparent generality of the results support the hypothesis that the geographical distribution of the feedback parameter is a basic and robust feature of the climate system and importantly determines the response to forcing.

10 Summary

Results from climate change simulations with a variety of GCMs indicate that global mean temperature change is proportional to the global mean radiative forcing, broadly independent of the nature and pattern of the forcing. The "constant" of proportionality measures the climate sensitivity. Simulation results also reveal several notable features of the geographical temperature response namely that: the temperature response patterns generally do not resemble the forcing patterns; there is a tendency for a "generic" temperature response pattern independent of the forcing but that this does not hold for all forcing patterns, especially for those with sharp gradients of forcing; nevertheless, temperature patterns show a remarkable linearity or additivity whereby the sum of response patterns for different forcings is closely the response pattern for the sum of the forcings.

Aspects of climate sensitivity are reviewed in terms of the vertically integrated energy budget equation for the climate system. The local contribution to the global feedback/sensitivity is evaluated from CCCma GCM simulations and its geographical pattern displayed. The model exhibits regions of positive feedback over high latitude oceans, over northern land areas, and over the equatorial Pacific in association with the mean El Nino response simulated in the model. The remaining regions over oceans and tropical land areas exhibit negative feedback. Of course the overall global feedback must be negative.

The feedback parameter is decomposed into components associated with short- and long-wave radiative processes and with cloud-free atmosphere/surface and cloud feedbacks. All of the feedback components display regions of both positive and negative values with the exception of the solar clear-sky/surface component which is positive over high-latitude oceans and northern land as a consequence of the positive albedo feedback associated with the retreat of ice and snow cover. The feedback results are not dominated by any one component or process but all components vary from place to place so that there is no simple physical picture that applies everywhere.

The nature and distribution of the feedback parameter that is diagnosed, together with the relationships between forcing and response summarized above, supports a feedback/response hypothesis which states that, to first order, climate response patterns are determined by the geographical pattern of local feedback processes. The argument is that robust local feedback processes act not only on local forcing changes but also on remote forcing changes which are felt locally via system transport changes. The feedback processes act to *localize* forcing changes and to generate a temperature response pattern which depends firstly on the pattern of feedbacks and only secondarily on the pattern of the forcing. The implication is that the geographical distribution of feedback processes, measured by the feedback parameter λ, can be regarded as a feature of the climate model (and by inference of the climate system) and not a (or only a comparatively weak) function of temperature, forcing, or climate state. Transport changes are a reactive intermediary between forcing and feedback and dynamical processes do not play the determining role in the response.

A zonally averaged illustrative model based on the hypothesis qualitatively reproduces the kinds of forcing/temperature response behaviour seen in the CCCma GCM and in other GCMs. More generally, it is shown that the additivity of temperature patterns follows as a consequence of the hypothesis, i.e. as a consequence of the robustness of λ together with the extent to which transport changes are a linear function of temperature change.

If the geographical pattern of the feedback parameter λ is a feature of the climate system, the "constant" of proportionality between global mean temperature and forcing change, measuring the climate sensitivity, is generally not constant and depends on the particular temperature response pattern and hence, indirectly, on the nature and pattern of the forcing. This dependence is not strong however, and the tendency for a "generic" temperature response to a range of common forcings is reflected in the comparative constancy of the sensitivity parameter.

The geographic distribution of λ indicates that some regions are more responsive to local and remote forcing changes than others. Anthropogenic or natural forcing changes will preferentially affect these regions, even if the forcing changes are comparatively remote. Additionally, modest forcing changes (of either sign) which act in regions of positive feedback will produce a comparatively large response both locally and globally. The distribution of local feedback processes, characterized by the feedback parameter, is an important determinant

of the pattern and magnitude of temperature response in that the feedbacks ''localize'' the response to forcing, even forcing that is remote.

Acknowledgements We greatly appreciate the work of Dave Ramsden, Cathy Reader, Warren Lee, Greg Flato and others in the production of the model results analyzed here. D. Robataille reran part of the simulations to obtain the cloud forcing results. We also thank John Fyfe and John Scinocca for their helpful comments.

References

Boer GJ (1993) Climate change and the regulation of the surface moisture and energy budgets. Clim Dyn 8: 225–239

Boer GJ (1995) Some dynamical consequences of greenhouse gas warming. Atmos-Ocean 33: 731–751

Boer GJ, Flato G, Reader MC, Ramsden D (2000a) A transient climate change simulation with greenhouse gas and aerosol forcing: experimental design and comparison with the instrumental record for the twentieth century. Clim Dyn 16: 405–425

Boer GJ, Flato G, Ramsden D (2000b) A transient climate change simulation with green-house gas and aerosol forcing: projected climate for the twenty first century. Clim Dyn 16: 427–450

Chen C-T, Ramaswamy V (1996a) Sensitivity of simulated global climate to perturbation in low cloud microphysical properties. Part I: globally uniform perturbations. J Clim 9: 1385–1402

Chen C-T, Ramaswamy V (1996b) Sensitivity of simulated global climate to perturbation in low cloud microphysical properties. Part II: spatially localized perturbations. J Clim 9: 2788–2801

Colman RA, Power S, McAvaney B (1997) Non-linear climate feedback analysis in an atmospheric general circulation model. Clim Dyn 13: 717–731

Flato G, Boer GJ, Lee W, McFarlane N, Ramsden D, Weaver A (2000) The CCCma global coupled model and its climate. Clim Dyn 16: 451–467

Forster P, Blackburn M, Glover R, Shine K (2000) An examination of climate sensitivity for idealized climate change experiments in an intermediate general circulation model. Clim Dyn 16: 833–849

Hansen J, Lacis A, Rind D, Russell G, Stone P, Fung I, Ruedy R, Learner J (1984) Climate sensitivity: analysis of feedback mechanisms. In: Climate processes and climate sensitivity. Geophys Monogr Ser, 29, 130–163. AGU, Washington, D.C., USA

Hansen J, Sato M, Ruedy R (1997) Radiative forcing and climate response. J Geophysical Res 192: 6831–6864

IPCC (2001) Climate change 2001, the scientific basis. Cambridge University Press, Cambridge, UK, pp 881

Meehl GA, Washington WM (1996) EI Niño-like climate change in a model with increased atmospheric CO_2 concentrations. Nature 382: 56–60

Murphy JM (1995) Transient response of the Hadley Centre coupled ocean-atmosphere model to increasing carbon dioxide: Part III. analysis of global-mean response using simple models. J Clim 8: 57–80

Pacanowski RC, Dixon K, Rosati A (1993) The GFDL modular ocean model users guide. GFDL Ocean Group Tech Rep 2. GFDL, Princeton, pp 46

Palmer TN (1999) A nonlinear dynamical perspective on climate prediction. J Clim 12: 575–591

Ramanathan V, Collins W (1991) Thermodynamic regulation of ocean warming by cirrus clouds deduced from the 1987 El Niño. Nature 351: 27–32

Raper S, Gregory J, Stouffer R (2002) The role of climate sensitivity and ocean heat uptake on AOGCM transient temperature response. J Clim 15: 124–130

Reader M, Boer GJ (1998) The modification of green house gas warming by the direct effect of sulphate aerosols. Clim Dyn 14: 593–607

Senior CA, Mitchell J (2000) The time-dependence of climate sensitivity. Geophys Res Lett 27: 2685–2689

Shapiro R (1971) Smoothing, filtering and boundary effects. Rev Geophys Space Phys 8: 359–387

Shine K, Fouquart Y, Ramaswamy V, Solomon S, Srinivasan J (1995) Chapter 4, Climate change 1994; radiative forcing of climate change, Chapter 4. Cambridge University Press, Cambridge

Stocker T, Wright D, Mysak L (1992) A zonally averaged, coupled ocean-atmosphere model for paleoclimate studies. J Clim 5: 773–797

Watterson IG (2000) Interpretation of simulated global warming using a simple model. J Clim 13: 202–215

Wetherald R, Manabe S (1988) Cloud feedback processes in a general circulation model. J Atmos Sci 45: 1397–1415

Yu B, Boer GJ (2002) The roles of radiation and dynamical processes in the El Nino-like response to global warming. Clim Dyn 19: 539–553

Zhang M, Kiehl J, Hack J (1996) Cloud-radiative feedback as produced by different parameterization of cloud emissivity in CCM2. NATO ASI Series, Springer, Berlin Heidelberg New York, pp 213–228